Structural Dynamic Response under Uncertainty - An Interval Finite Element Approach

Naijia Xiao[1)], Francesco Fedele[2)] and Rafi Muhanna[1)]
[1)] *School of Civil and Environmental Engineering, Georgia Institute of Technology, Atlanta, GA 30332, USA, {naijia.xiao, rafi.muhanna}@gatech.edu*
[2)] *School of Civil and Environmental Engineering and School of Electrical and Computer Engineering, Georgia Institute of Technology, Atlanta, GA 30332, USA, fedele@gatech.edu*

Abstract: An analysis of the structural dynamic response under uncertainty is presented. Uncertainties in load and material are modeled as intervals exploiting the interval finite element method (IFEM). To reduce overestimation and increase the computational efficiency of the solution, we do not solve the dynamic problem by an explicit step-by-step time integration scheme. Instead, our approach solves for the structural variables in the whole time domain simultaneously by an implicit scheme using discrete Fourier transform and its inverse (DFT and IDFT). Non-trivial initial conditions are handled by modifying the right-hand side of the governing equation. To further reduce overestimation, a new decomposition strategy is applied to the IFEM matrices, and both primary and derived quantities are solved simultaneously. The final solution is obtained using an iterative enclosure method, and in our numerical examples the exact solution is enclosed at minimal computational cost.

Keywords: interval finite element method, dynamic response, discrete Fourier transform, matrix decomposition, iterative enclosure method

1. Introduction

For any given physical system, uncertainties caused by measurement device or environmental conditions in the data acquisition process causes inconsistencies between the estimated and actual system behavior (Fernández-Martínez et al., 2013). Thus it is necessary to model and track the propagation of uncertainties in the system and to reliably evaluate the accuracy of the obtained solution. Conventional treatment of uncertainties involves the probability theory (Lutes and Sarkani, 2004), in which random variables are used to model the uncertainties encountered. In cases where enough measurement data is available and sufficient to reliably predict the nature of the uncertainties, probability approach is preferred. However, when there is not enough measurement data (Moens and Hanss, 2011; Zhang, 2005), as an alternative, one can turn to other available non-probabilistic approaches, such as Bayesian networks (Igusa et al., 2002; Soize, 2013; Unger and Könke, 2011), fuzzy sets (Adhikari and Khodaparast, 2014; Dehghan et al., 2006; Erdogan and Bakir, 2013; Klir and Wierman, 1999), evidence theory (Bai et al., 2013; Dempster, 1967; Jiang et al., 2013; Shafer, 1968), and intervals (Corliss et al., 2007; Do et al., 2014; Impollonia and Muscolino, 2011; Muhanna et al., 2007). Here the interval approach is adopted, in which uncertainties are modeled by interval

numbers characterized by their respective lower and upper bounds. More discussions on intervals and interval arithmetic can be found in Alefeld and Herzberger (1984), Kulisch and Miranker (1981), and Moore et al. (2009).

In this paper, an interval-based approach for the analysis of structural dynamic problems in the time domain is presented. In particular, the time-domain dynamics of elastic structures with uncertain geometric and material properties are studied. Uncertain parameter of the structure are modeled by intervals, and Interval Finite Element Method (IFEM) is implemented (Hu and Qiu, 2010; Qiu and Ni, 2010; To, 2012; Xia et al., 2010). The structure is governed by the following interval differential equation in the time domain,

$$\mathbf{K}\mathbf{u} + \mathbf{C}\dot{\mathbf{u}} + \mathbf{M}\ddot{\mathbf{u}} = \mathbf{f}, \tag{1}$$

where $\mathbf{K}$, $\mathbf{C}$, and $\mathbf{M}$ are respectively the stiffness, damping, and mass matrix of the structure, $\mathbf{u}$ is the unknown nodal displacement vector, $\dot{\mathbf{u}}$ and $\ddot{\mathbf{u}}$ are the corresponding nodal velocity and acceleration vector, $\mathbf{f}$ is the time-varying nodal equivalent load. From now on, *non-italic bold letters are used to denote interval variables.* The initial conditions are expressed in an interval form,

$$\mathbf{u}(0) = \mathbf{u}_0, \qquad \dot{\mathbf{u}}(0) = \mathbf{v}_0, \tag{2}$$

where $\mathbf{u}_0$ and $\mathbf{v}_0$ are the initial nodal displacement and velocity vector, respectively.

In practice, the differential Eq. (1) is solved at discrete time t_k, which are usually uniformly spaced in time. Conventional numerical integration approaches solve Eq. (1) recursively, viz. the solution at the current time t_k is obtained by using the solution in the previous time t_{k-1}. One notable example of the numerical integration method in structural analysis is the Newmark-β method (De Borst et al., 2012; Dokainish and Subbaraj, 1989; Paz, 1997). However, such recursive approach is not directly applicable for IFEM implementation, because overestimation due to interval dependency accumulates, and the yielded interval enclosure quickly become excessively wide and practically useless after a few iterations in time.

Alternatively, the transformation approach can be used (Bae et al., 2014; Yang et al., 2012). In the current method, the Discrete Fourier Transform (DFT) approach is adopted. A brief introduction on the DFT can be found in Santamarina and Fratta (2005). The governing Eq. (1) is transformed into the frequency domain using DFT, and the computed response is expressed back into the time domain using the corresponding inverse transform (Inverse Discrete Fourier Transform, IDFT). As a result, the solution vector at all time steps are obtained simultaneously.

In the following sections, first the deterministic solver based on the DFT approach is presented. Then the presented interval solver is introduced in detail. The governing Eq. (1) is reintroduced into a fixed-point form, and an iterative approach is adopted to obtain a sharp interval enclosure of the exact solution. Finally, the performance of the current method is compared with other available methods in a few numerical example.

2. Deterministic Dynamic Solver

In this section, the deterministic dynamic solver based on the DFT approach (Veletsos and Kumar, 1983; Veletsos and Ventura, 1985) is presented. The dynamic response of a linearly elastic structure is studied, which, after FEM discretization, is governed by

$$Ku + C\dot{u} + M\ddot{u} = f, \tag{3}$$

where K, C, and M are the stiffness, damping, and mass matrices of the structure, respectively, u is the nodal displacement vector, $\dot{u}$ and $\ddot{u}$ are the first and second derivatives of u with respect to the time (or, equivalently, nodal velocity and acceleration), and f is the nodal equivalent load. The initial condition is given by

$$u(0) = u_0, \qquad \dot{u}(0) = v_0. \tag{4}$$

The system is assumed discretized in time. The nodal equivalent load at discrete time t_k is given, and the goal is to solve for the nodal displacement vector u at t_k, as well as its derivatives $\dot{u}$ and $\ddot{u}$. That is, $f(t_k) = f_k,\ u(t_k) = u_k,\ \dot{u}(t_k) = \dot{u}_k,\ \ddot{u}(t_k) = \ddot{u}_k$. Usually, the time steps are uniformly spaced, viz. $t_k = k\Delta t$. The sampling interval Δt must be small enough to prevent any potential aliasing (Santamarina and Fratta, 2005). Let T be the total time length of the signal and N the total number, then $T = N\Delta t$.

In the discrete Fourier transform approach, DFT is applied to the discrete version of the governing Eq. (3) and transform it into

$$\left(-\omega_j^2 M + i\omega_j C + K\right) \mathcal{F}_t(u)_j = \mathcal{F}_t(f)_j, \tag{5}$$

where $i = \sqrt{-1}$ is the imaginary unit, $\omega_j = j\Delta\omega$ with $\Delta\omega = 2\pi/T$ being the fundamental frequency, $\mathcal{F}_t(u)_j$ and $\mathcal{F}_t(f)_j$ are the Fourier transform of the nodal displacement u_k and equivalent load f_k, respectively. Then the nodal displacement vector in the time-domain is obtained by applying the IDFT to $\mathcal{F}_t(u)_j$, viz.

$$u_n = \frac{1}{N}\sum_{j=0}^{N-1} \mathcal{F}_t(u)_j e^{-i(2\pi/N)jn} = \frac{1}{N}\sum_{j=0}^{N-1} G_j \mathcal{F}_t(f)_j e^{-i(2\pi/N)jn}, \tag{6}$$

where G_j is the inverse of the effective stiffness matrix in Eq. (5). To ensure that the final solution u_n is real, i.e., null imaginary part, G_j takes the following form,

$$G_j = \begin{cases} \left(-\omega_j^2 M + i\omega_j C + K\right)^{-1}, & 0 \le j < N/2; \\ \text{conjugate of } G_{N-j}, & N/2 \le j < N. \end{cases} \tag{7}$$

The above approach essentially solves for the stationary response of the structure caused by periodic loads with period T. The results are identical to the actual dynamic response with trivial initial conditions ($u_0 = v_0 = 0$) when enough zero-padding is attached. The length of the zero-padding, T_p, can be estimated from

$$e^{-\zeta\omega T_p} < \tau_{err}, \qquad \Rightarrow \qquad T_p > \frac{\ln \tau_{err}}{\zeta\omega}, \tag{8}$$

where τ_{err} is the error tolerance, ω is the lowest natural frequency of the structure, and ζ is the corresponding effective damping ratio. Let T_0 be the length of the original signal, then $T = T_0 + T_p$.

Non-trivial initial conditions can be modeled by modifying the equivalent load (Lee et al., 2005; Liu et al., 2015; Mansur et al., 2000). For initial displacement u_0, it is equivalent to add a constant load $f_{u0} = Ku_0$, which exist for the time interval $T_0 \leq t < T$. For initial velocity v_0, it is equivalent to add an impulse load $f_{v0} = Mv_0/\Delta t$, at time $t = 0$ for a duration of time Δt.

3. Interval Dynamic Solver

Assume the elastic structure under study contains uncertain parameters, which are modeled by intervals. The structural system is governed by Eqs. (1) and (2). For simplicity, the Rayleigh damping is adopted. The damping matrix

$$\mathbf{C} = \alpha_d \mathbf{M} + \beta_d \mathbf{K}, \tag{9}$$

where α_d and β_d are the Rayleigh damping coefficients. To reduce overestimation due to interval dependency, the interval matrix decomposition outlined before is adopted. Then DFT is used to transform the governing equation into a fixed-point form, which is further solved by a new variant of iterative enclosure method. Details on the current method are presented in the following subsections.

3.1. Interval matrix decomposition

The matrix decomposition strategy reduces overestimation due to interval dependency by avoiding multiple occurrences of the same interval variable in the formulation. The stiffness matrix $\mathbf{K}$, the mass matrix $\mathbf{M}$, and the stress-displacement matrix $\mathbf{S}$ are decomposed into

$$\mathbf{K} = A\mathrm{diag}(\Lambda\boldsymbol{\alpha})A^T, \qquad \mathbf{M} = A_m\mathrm{diag}(\Lambda_m\boldsymbol{\alpha}_m)A_m^T, \tag{10}$$

where A, Λ, A_m, and Λ_m are deterministic matrices, $\boldsymbol{\alpha}$ is the interval stiffness parameter vector that accounts for uncertainties in the stiffness matrix $\mathbf{K}$, and $\boldsymbol{\alpha}_m$ is the interval mass parameter vector that accounts for uncertainties in the mass matrix $\mathbf{M}$.

By combining the nodal equivalent load vector $\mathbf{f}_k$ at different time steps t_k, the interval load matrix $\mathbf{f}$ is obtained, whose k-th column is $\mathbf{f}_k$. When the structure is subject to external loading and the M-$\boldsymbol{\delta}$ method is adopted (Muhanna and Mullen, 2001), $\mathbf{f}$ is decomposed into

$$\mathbf{f} = F\boldsymbol{\delta}_t, \tag{11}$$

where F is a deterministic matrix, and $\boldsymbol{\delta}_t$ is the time-varying load uncertainty matrix. Usually it is necessary to distinguish the uncertainty in the magnitude of the load and the uncertainty in the time-history of the load. Thus $\boldsymbol{\delta}_t$ is further decomposed into an interval column vector $\boldsymbol{\delta}$ and an interval row vector $\mathbf{d}_t$, viz. $\boldsymbol{\delta}_t = \boldsymbol{\delta}\mathbf{d}_t$, where $\boldsymbol{\delta}$ models the uncertainties in the load magnitude and $\mathbf{d}_t$ models the uncertainties in the load time-history. Finally, the nodal equivalent load $\mathbf{f}$ is decomposed into

$$\mathbf{f} = (F\boldsymbol{\delta})\mathbf{d}_t. \tag{12}$$

Similarly, when the structure is subject to ground motion, $\mathbf{f}$ is decomposed into

$$\mathbf{f} = -\mathbf{M}\mathbf{a} = -\mathbf{M}q\boldsymbol{\delta}_t, \tag{13}$$

where $\boldsymbol{\delta}_t$ denotes the time-varying ground acceleration, $\mathbf{a}$ represents the resulting nodal acceleration of the structure, and q relates $\boldsymbol{\delta}_t$ to $\mathbf{a}$, viz. $\mathbf{a} = q\boldsymbol{\delta}_t$. By using the same decomposition for $\boldsymbol{\delta}_t$, and noting Eq. (10),

$$\mathbf{f} = -A_m \mathrm{diag}(\Lambda_m \boldsymbol{\alpha}_m) A_m^T q \boldsymbol{\delta} \mathbf{d}_t = A_m \left(\Lambda_m \boldsymbol{\alpha}_m \circ B_f \boldsymbol{\delta}\right) \mathbf{d}_t, \tag{14}$$

where $B_f = -A_m^T q$, and $a \circ b$ is the element-by-element Hadamard product of two vectors a and b.

When the initial conditions are non-trivial and modeled by intervals, as shown in Eq. (2), the corresponding nodal equivalent load $\mathbf{f}$ is given by

$$\mathbf{f} = \mathbf{K}\mathbf{u}_0 d_{u_0} + \mathbf{M}\mathbf{v}_0 d_{v_0}, \tag{15}$$

where d_{u_0} and d_{v_0} are two deterministic row vectors. d_{u_0} is zero for the time interval $0 \le t_k < T_0$ and unity for the time interval $T_0 \le t_k < T$, where T_0 and T are the length of the original and padded signal. d_{v_0} represents an impulse load which is $1/\Delta t$ at $t_k = 0$ and zero everywhere else. Noting the decomposition in Eq. (10),

$$\mathbf{f} = A\left(\Lambda\boldsymbol{\alpha} \circ A^T \mathbf{u}_0\right) d_{u_0} + A_m \left(\Lambda_m \boldsymbol{\alpha}_m \circ A_m^T \mathbf{v}_0\right) d_{v_0}, \tag{16}$$

which has a similar matrix form as Eq. (14). Thus the non-trivial initial conditions are treated in the same manner as ground accelerations.

3.2. Interval governing equations

To solve the interval differential Eq. (1), following the DFT approach outlined in Section 2, the equation is transformed into the frequency domain, viz.

$$\left(-\omega_j^2 \mathbf{M} + i\omega_j \mathbf{C} + \mathbf{K}\right) \mathcal{F}_t(\mathbf{u})_j = \mathcal{F}_t(\mathbf{f})_j, \tag{17}$$

where $\mathcal{F}_t(\mathbf{u})_j$ and $\mathcal{F}_t(\mathbf{f})_j$ are the Fourier transform of the nodal displacement $\mathbf{u}_k$ and equivalent load $\mathbf{f}_k$, respectively.

To include compatibility requirements and essential boundary conditions in the governing equation, and to ensure that the final solution has zero imaginary part, Eq. (17) is brought into the following equivalent form,

$$\begin{Bmatrix} \mathbf{K}_{\mathrm{eff},j} & C^T \\ C & 0 \end{Bmatrix} \begin{Bmatrix} \mathcal{F}_t(\mathbf{u})_j \\ \mathcal{F}_t(\boldsymbol{\lambda})_j \end{Bmatrix} = \begin{Bmatrix} \mathcal{F}_t(\mathbf{f})_j \\ 0 \end{Bmatrix}, \tag{18}$$

where $\mathbf{K}_{\mathrm{eff},j}$ is the effective stiffness matrix corresponding to the j-th frequency ω_j, namely

$$\mathbf{K}_{\mathrm{eff},j} = \begin{cases} -\omega_j^2 \mathbf{M} + i\omega_j \mathbf{C} + \mathbf{K}, & 0 \le j < N/2; \\ \text{conjugate of } \mathbf{K}_{\mathrm{eff},N-j}, & N/2 \le j < N, \end{cases} \tag{19}$$

C is the constraint matrix that imposes compatibility requirements and essential boundary conditions, and $\boldsymbol{\lambda}_k$ is the Lagrangian multiplier representing the internal forces and support reactions at t_k. By adopting the Rayleigh damping and the decomposition of $\mathbf{K}$ and $\mathbf{M}$ in Eq. (10), $\mathbf{K}_{\text{eff},j}$ can be decomposed into

$$\mathbf{K}_{\text{eff},j} = A_{\text{eff},j}\text{diag}\left(\Lambda_{\text{eff}}\boldsymbol{\alpha}_{\text{eff}}\right)B_{\text{eff}}, \tag{20}$$

where $A_{\text{eff},j}$ is a deterministic matrix depending on the frequency ω_j,

$$A_{\text{eff},j} = \begin{cases} \left\{(1+ib\omega_k)A \quad (-\omega_k^2 + ia\omega_k)A_m\right\}, & 0 \le j < N/2; \\ \text{conjugate of } A_{\text{eff},N-j}, & N/2 \le j < N, \end{cases} \tag{21}$$

and Λ_{eff}, B_{eff}, and $\boldsymbol{\alpha}_{\text{eff}}$ are time-invariant variables,

$$\Lambda_{\text{eff}} = \begin{Bmatrix} \Lambda & 0 \\ 0 & \Lambda_m \end{Bmatrix}, \quad B_{\text{eff}} = \begin{Bmatrix} A^T \\ A_m^T \end{Bmatrix}, \quad \boldsymbol{\alpha}_{\text{eff}} = \begin{Bmatrix} \boldsymbol{\alpha} \\ \boldsymbol{\alpha}_m \end{Bmatrix}. \tag{22}$$

Suppose the structure is subject to external loading, then

$$\mathcal{F}_t(\mathbf{f})_j = \mathcal{F}_t(F\boldsymbol{\delta}\mathbf{d}_t)_j = F\boldsymbol{\delta}\mathcal{F}_t(\mathbf{d}_t)_j. \tag{23}$$

Then Eq. (18) is equivalent to the following decomposed form

$$\begin{Bmatrix} K_{\text{eff},j0} & C^T \\ C & 0 \end{Bmatrix}\begin{Bmatrix} \mathcal{F}_t(\mathbf{u})_j \\ \mathcal{F}_t(\boldsymbol{\lambda})_j \end{Bmatrix} = \begin{Bmatrix} F \\ 0 \end{Bmatrix}\boldsymbol{\delta}\mathcal{F}_t(\mathbf{d}_t)_j - \begin{Bmatrix} A_{\text{eff},j} \\ 0 \end{Bmatrix}\text{diag}\Big(B_{\text{eff}}\mathcal{F}_t(\mathbf{u})_j\Big)\Lambda_{\text{eff}}\Delta\boldsymbol{\alpha}_{\text{eff}}, \tag{24}$$

by using the decomposition in Eqs. (20) and (23) and the following identities

$$\begin{aligned} A_{\text{eff},j}\text{diag}\left(\Lambda_{\text{eff}}\boldsymbol{\alpha}_{\text{eff}}\right)B_{\text{eff}}\mathcal{F}_t(\mathbf{u})_j &= A_{\text{eff},j}\Big(\Lambda_{\text{eff}}\boldsymbol{\alpha}_{\text{eff}} \circ B_{\text{eff}}\mathcal{F}_t(\mathbf{u})_j\Big) \\ &= A_{\text{eff},j}\text{diag}\Big(B_{\text{eff}}\mathcal{F}_t(\mathbf{u})_j\Big)\Lambda_{\text{eff}}\boldsymbol{\alpha}_{\text{eff}}, \end{aligned} \tag{25}$$

where $\Delta\boldsymbol{\alpha}_{\text{eff}}$ is the difference between $\boldsymbol{\alpha}_{\text{eff}}$ and the reference vector $\alpha_{\text{eff}0}$, viz. $\Delta\boldsymbol{\alpha}_{\text{eff}} = \boldsymbol{\alpha}_{\text{eff}} - \alpha_{\text{eff}0}$, and $K_{\text{eff},j0} = A_{\text{eff},j}\text{diag}(\Lambda_{\text{eff}}\alpha_{\text{eff}0})B_{\text{eff}}$.

When the structure is subject to ground motion, according to Eq. (14),

$$\begin{aligned} \mathcal{F}_t(\mathbf{f})_j &= A_f\left(\Lambda_m\boldsymbol{\alpha}_m \circ B_f\boldsymbol{\delta}\right)\mathcal{F}_t(\mathbf{d}_t)_j \\ &= \left(A_f\left(\Lambda_m\alpha_{m0} \circ B_f\boldsymbol{\delta}\right) + A_f\left(\Lambda_m\Delta\boldsymbol{\alpha}_m \circ B_f\boldsymbol{\delta}\right)\right)\mathcal{F}_t(\mathbf{d}_t)_j \\ &= F_0\boldsymbol{\delta}\mathcal{F}_t(\mathbf{d}_t)_j + A_f\text{diag}\Big(B_f\boldsymbol{\delta}\mathcal{F}_t(\mathbf{d}_t)_j\Big)\Lambda_m\Delta\boldsymbol{\alpha}_m, \end{aligned} \tag{26}$$

where $\Delta\boldsymbol{\alpha}_m$ is the difference between $\boldsymbol{\alpha}_m$ and the reference vector α_{m0}, viz. $\Delta\boldsymbol{\alpha}_m = \boldsymbol{\alpha}_m - \alpha_{m0}$, and $F_0 = A_f\text{diag}(\Lambda_m\alpha_{m0})B_f$. Then the generalized equivalent load in Eq. (18) is decomposed into

$$\begin{Bmatrix} \mathcal{F}_t(\mathbf{f})_j \\ 0 \end{Bmatrix} = \begin{Bmatrix} F_0 \\ 0 \end{Bmatrix}\boldsymbol{\delta}\mathcal{F}_t(\mathbf{d}_t)_j + \begin{Bmatrix} A_f \\ 0 \end{Bmatrix}\text{diag}\Big(B_f\boldsymbol{\delta}\mathcal{F}_t(\mathbf{d}_t)_j\Big)\Lambda_m\Delta\boldsymbol{\alpha}_m, \tag{27}$$

Eq. (18) is equivalent to the following decomposed form

$$\begin{Bmatrix} K_{\text{eff},j0} & C^T \\ C & 0 \end{Bmatrix} \begin{Bmatrix} \mathcal{F}_t(\mathbf{u})_j \\ \mathcal{F}_t(\boldsymbol{\lambda})_j \end{Bmatrix} = \begin{Bmatrix} F_0 \\ 0 \end{Bmatrix} \boldsymbol{\delta} \mathcal{F}_t(\mathbf{d}_t)_j \\ - \begin{Bmatrix} A_{\text{eff}} & A_f \\ 0 & 0 \end{Bmatrix} \text{diag}\left(\begin{Bmatrix} B_{\text{eff}} \mathcal{F}_t(\mathbf{u})_j \\ -B_f \boldsymbol{\delta} \mathcal{F}_t(\mathbf{d}_t)_j \end{Bmatrix} \right) \begin{Bmatrix} \Lambda_{\text{eff}} & \\ 0 & \Lambda_m \end{Bmatrix} \Delta\boldsymbol{\alpha}_{\text{eff}}. \tag{28}$$

Due to the similarities between the decomposition of the equivalent load in Eqs. (14) and (16), the above formulation can be extended to cases when the initial conditions are non-trivial.

3.3. Iterative enclosure method

To solve the interval linear system Eqs. (24) and (28), they are recast into the following form

$$K_{g,j} \mathcal{F}_t(\mathbf{u}_g)_j = F_g \boldsymbol{\delta} \mathcal{F}_t(\mathbf{d}_t)_j - A_{g,j} \text{diag}\Big(\mathcal{F}_t(\mathbf{v}_g)_j \Big) \Lambda_g \Delta\boldsymbol{\alpha}_{\text{eff}}, \tag{29}$$

where $K_{g,j}$, F_g, $A_{g,j}$, Λ_g are given deterministic matrices, $\mathbf{u}_g$ is the unknown interval vector, $\boldsymbol{\delta}$, $\mathbf{d}_t$, and $\Delta\boldsymbol{\alpha}_{\text{eff}}$ are given interval vectors, and $\mathbf{v}_g$ linearly depend on $\mathbf{u}_g$, viz. $\mathbf{v}_g = \mathbf{v}_0 + B_g \mathbf{u}_g$. Here subscripts $_j$ denotes variables associated with the j-th frequency ω_j. Note that matrices $K_{g,j}$ and $A_{g,j}$ are functions of the frequency ω_j. In the most general case, $\mathbf{u}_g$ includes $\mathbf{u}$ and $\boldsymbol{\lambda}$, and the auxiliary variable $\mathbf{v}_g$ includes $B_{\text{eff}}\mathbf{u}$, $-B_f\boldsymbol{\delta}\mathbf{d}_t$, and $A_s^T\mathbf{u}$.

Now introduce $G_j = K_{g,j}^{-1}$. Multiplying both sides of Eq. (29) by G_j yields

$$\mathcal{F}_t(\mathbf{u}_g)_j = (G_j F_g) \boldsymbol{\delta} \mathcal{F}_t(\mathbf{d}_t)_j - (G_j A_{g,j}) \text{diag}\Big(\mathcal{F}_t(\mathbf{v}_g)_j \Big) \Lambda_g \Delta\boldsymbol{\alpha}_{\text{eff}}. \tag{30}$$

Then $\mathbf{u}_g$ is obtained by applying the IDFT to both side of (30),

$$\mathbf{u}_{g,k} = \Big(\mathcal{F}_t^{-1}(G_j F_g) * \mathbf{d}_t \Big)_k \boldsymbol{\delta} - \Big(\mathcal{F}_t^{-1}(G_j A_{g,j}) * \text{diag}(\mathbf{v}_g) \Big)_k \Lambda_g \Delta\boldsymbol{\alpha}_{\text{eff}}, \tag{31}$$

where $(a*b)_k$ denotes the convolution between two discrete signals a_k and b_k. Eq. (31) can be recast into the following summation form,

$$\mathbf{u}_{g,k} = \left(\sum_{l=0}^{N-1} \mathcal{F}_t^{-1}(G_j F_g)_{k-l} \mathbf{d}_{t,l} \right) \boldsymbol{\delta} - \left(\sum_{l=0}^{N-1} \mathcal{F}_t^{-1}(G_j A_{g,j})_{k-l} \text{diag}(\mathbf{v}_{g,l}) \right) \Lambda_g \Delta\boldsymbol{\alpha}_{\text{eff}}. \tag{32}$$

Then a fixed-point form for $\mathbf{v}_{g,k}$ is obtained as

$$\mathbf{v}_{g,k} = \mathbf{v}_{0,k} + B_g \Big(\mathcal{F}_t^{-1}(G_j F_g) * \mathbf{d}_t \Big)_k \boldsymbol{\delta} - B_g \Big(\mathcal{F}_t^{-1}(G_j A_{g,j}) * \text{diag}(\mathbf{v}_g) \Big)_k \Lambda_g \Delta\boldsymbol{\alpha}_{\text{eff}}. \tag{33}$$

A guaranteed outer enclosure for $\mathbf{v}_{g,k}$ is obtained by iteratively using Eq. (33), starting from the trivial initial guess $\mathbf{v}_{g,k}^1 = \mathbf{v}_{0,k} + \big(\mathcal{F}_t^{-1}(G_j F_g) * \mathbf{d}_t \big)_k \boldsymbol{\delta}$. The iteration stops when no improvement in $\mathbf{v}_{g,k}^j$ is observed for two consecutive iterations, and the converged solution is denoted as $\mathbf{v}_{g,k}^n$. Then the outer solution $\mathbf{u}_{g,k}^{out}$ is obtained by substituting $\mathbf{v}_{g,k}$ in Eq. (31) with the converged solution $\mathbf{v}_{g,k}^n$.

The convolution between a deterministic signal and an interval signal is computed multiple times, as shown in Eqs. (31) and (33). To increase the computational efficiency and reduce overestimation in the final solution, the FFT-based fast interval convolution algorithm, proposed by Liu and Kreinovich (2010), is adopted. During the iteration in Eq. (33), only the radius of $\mathbf{v}_g$ is updated. All other vectors and matrices do not change after the first iteration.

4. Numerical Examples

The current IFEM algorithm is implemented using the interval MATLAB toolbox INTLAB (Rump, 1999). Interval enclosures of the structural responses of the following sample problems are calculated: *i*) a four-story rigid frame and *ii*) a simply supported truss. The performance of the current method is compared against other available methods in the literature: *i*) the endpoint combination method (EC) and *ii*) the Monte Carlo (MC) simulation. The results shows that the current method is applicable to the transient analysis of structural dynamic problems with uncertain parameters. Guaranteed interval enclosures of the exact structural responses in the time domain are obtained with small overestimations. In addition, the computational time is negligible when compared with other competing methods.

4.1. Four-story rigid frame

The first example is a four-story frame shown in Figure 1. The floors of the frame are assumed to be rigid enough to model the structure as an equivalent spring-mass system (shown in the right-hand side of Figure 1). The mass $\mathbf{m}_j$ and the inter-story shear stiffness $\mathbf{k}_j$ of each floor ($j = 1, \ldots, 4$) are modeled by independent interval variables, and given in Table I.

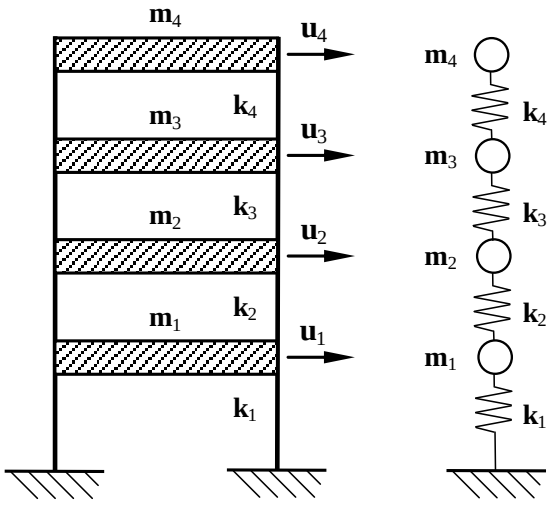

Figure 1. A four-story rigid frame and the equivalent spring-mass system.

Consider the structural response of the frame under a concentrated impact force acting on the top floor. The force has a duration of 4 s, and its variation during that time is deterministic, viz.

$$\mathbf{f}(t) = \begin{cases} \mathbf{P}\sin(\pi t/2), & 0 \le t \le 4 \text{ s}; \\ 0, & t > 4 \text{ s}, \end{cases} \tag{34}$$

where $\mathbf{P} = [0.99, 1.01]$ kN (2% uncertainty in the magnitude of the load). The damping matrix $\mathbf{C} = 0.5\mathbf{M} + 5 \times 10^{-3}\mathbf{K}$. The sampling rate is 100 Hz, so the sampling interval $\Delta t = 0.01$ s.

Figure 2 compares the lower and upper bounds of $\mathbf{u}_4$ for the first 10 s, obtained from the current method (IS, solid lines), Monte Carlo predictions (MC, dashed lines) from an ensemble of 10,000 simulations, the reference solution obtained from endpoint combination (EC, dash-dotted lines), and the deterministic solution (DS, dotted line). Note that IS always contains the reference solution EC, and MC is always contained by EC. In addition, the overestimation level of the current method

Table I. Interval mass and stiffness for the five-story rigid frame of Figure 1, including 1% uncertainties in mass, and 5% uncertainties in stiffness.

Floor	Mass (kg)			Stiffness (kN/m)		
	$\mathbf{m}_j$	mid $\mathbf{m}_j$	rad $\mathbf{m}_j$	$\mathbf{k}_j$	mid $\mathbf{k}_j$	rad $\mathbf{k}_j$
1	[5.416, 5.470]	5.443	0.027	[1.180, 1.240]	1.210	0.030
2	[5.416, 5.470]	5.443	0.027	[1.677, 1.763]	1.720	0.043
3	[5.416, 5.470]	5.443	0.027	[1.862, 1.958]	1.910	0.048
4	[5.416, 5.470]	5.443	0.027	[1.775, 1.865]	1.820	0.045

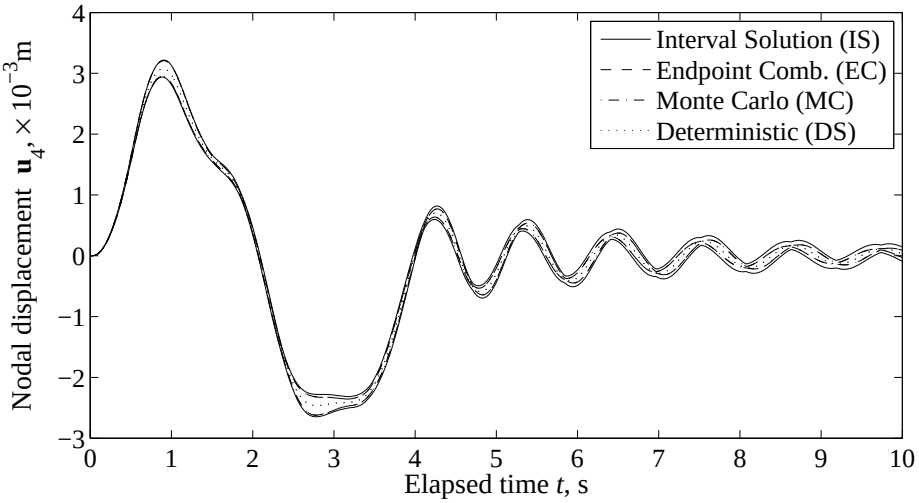

Figure 2. Lower and upper bounds of the nodal displacement $\mathbf{u}_4$ for the four-story frame of Figure 1 under a sinusoidal force: IS (solid lines) from the current method, EC (dashed lines), and MC (dash-dotted lines) from an ensemble of 10,000 simulations. Material uncertainty is 1% for mass, and 5% for stiffness. Load uncertainty is 2% for the magnitude.

slightly increases as the time increases. The MC solution is obtained using the DFT approach, which indistinguishable from the solution obtained from a recursive Newmark-β method.

Then the concentrated force $\mathbf{f}(t)$ is removed, and the structure is subject to non-trivial initial conditions. Figure 3 shows the nodal displacement $\mathbf{u}_4$ at the top floor for the first 10 s with non-trivial initial nodal displacement $\mathbf{u}_0$ (top) and nodal velocity $\mathbf{v}_0$ (bottom), respectively. Here 2%

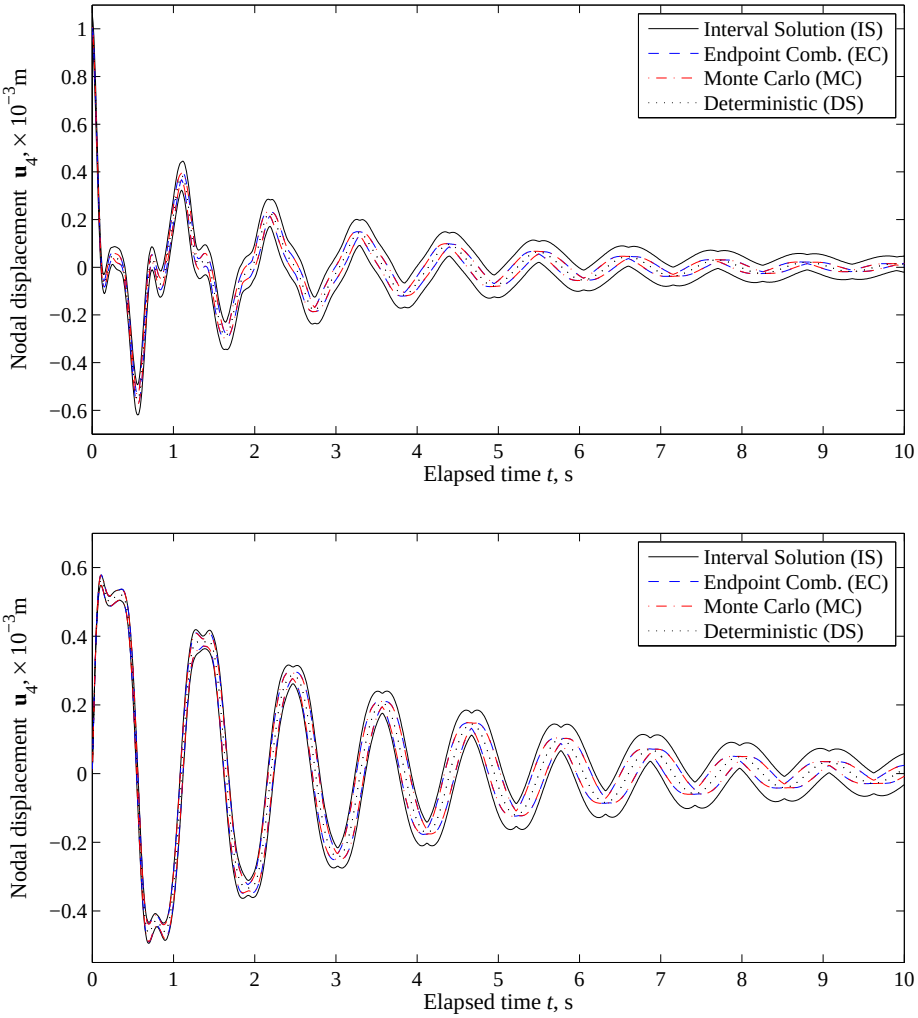

Figure 3. Lower and upper bounds of the nodal displacement $\mathbf{u}_4$ for the four-story frame of Figure 1 under non-trivial initial conditions: (top) non-trivial initial displacement $\mathbf{u}_0$, (bottom) non-trivial initial velocity $\mathbf{v}_0$. IS (black solid lines) from the current method, EC (blue dashed lines), and MC (red dash-dotted lines) from an ensemble of 10,000 simulations. Material uncertainty is 1% for mass, and 5% for stiffness. Uncertainty in the initial condition is 2% (see online version for colors).

uncertainty is considered for $\mathbf{u}_0$ and $\mathbf{v}_0$, viz.

$$\mathbf{u}_0 = \left\{ 0 \;\; 0 \;\; 0 \;\; 0 \;\; [0.99,\ 1.01] \right\}^T \times 10^{-3} \text{ m}; \tag{35}$$
$$\mathbf{v}_0 = \left\{ 0 \;\; 0 \;\; 0 \;\; 0 \;\; [0.99,\ 1.01] \right\}^T \times 10^{-2} \text{ m/s}.$$

Figure 3 shows that the high frequency components dissipate quickly. After about 3 s, the response of the structure is dominated by the lowest frequency vibration. Observe that the performance of the current method is the same as in the previous case. The obtained interval solution guarantees to enclose the reference solution (endpoint combination, EC), and the overestimation level increases slightly as the time increases. Thus non-trivial initial conditions are handled successfully.

4.2. Simply supported truss

The second example is a simply supported symmetric truss composed of 15 bars, as shown in Figure 4. The joints are labeled from 1 to 8, and the bars are labeled from 1 to 15. Time-varying concentrated load $\mathbf{P}$ acts at joint 5. Bars 1 to 3, 13 to 15 have the same cross section area $A = 1.0 \times 10^{-3}$ m^2, and all other bars, viz. bars 4 to 12, have smaller cross section area $A = 6.0 \times 10^{-4}$ m^2. All the bars are made of steel. They have the interval mass density $\boldsymbol{\rho}$ with midpoint value $\rho = 7.8 \times 10^3$ kg/m^3, and the interval Young's modulus $\mathbf{E}$ with midpoint value $E = 200$ GPa.

Fifteen bar elements are used to model the truss in Figure 4. Element mass density $\boldsymbol{\rho}$ and Young's modulus $\mathbf{E}$ are assumed independent, and they are modeled by 30 interval variables. The midpoint of the load $\mathbf{P}$ is a sinusoid with a frequency of 50 Hz and an amplitude of 200 kN, viz.

$$P = 200 \sin(100\pi t) \text{ kN}. \tag{36}$$

The damping matrix $\mathbf{C} = 20\mathbf{M} + 3 \times 10^{-5}\mathbf{K}$. The sampling rate is 10 kHz, so $\Delta t = 1 \times 10^{-4}$ s.

Then vertical displacement $\mathbf{v}_5$ at joint 5 is selected for comparison among the various methods mentioned previously. Consider 1% uncertainty for the magnitude and time-history of the load, as well as Young's modulus and mass density of each bar. Figure 5 plots the lower and upper

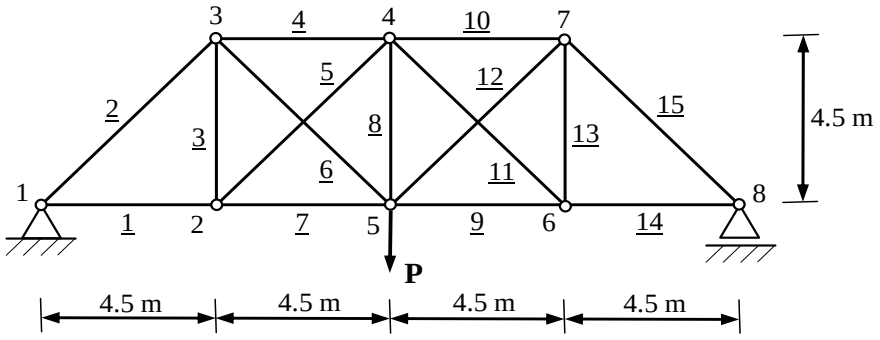

Figure 4. A simply supported symmetric truss subject to concentrated force.

bounds of $\mathbf{v}_5$ for the first 0.1 s obtained from the current method (IS, solid lines) and the Monte Carlo predictions (MC, dashed lines from the Newmark-β approach, and dash-dotted lines from the DFT approach) from an ensemble of 100,000 simulations. Observe that the current method obtains guaranteed enclosures of the MC prediction.

Figure 5 shows that the uncertainties in the structural responses increase significantly over time. This behavior is due to the fact that the load history uncertainties are modeled by independently varied intervals at different time steps. In the current example, this means 0.1 s $\times$ 10 kHz = 1,000 independent interval variables. As a result, the overall uncertainty level is much higher than 1%. This also explains the growing differences between IS and MC predictions over time. Figure 6 considers (top) 2% uncertainties in load time-history and (bottom) 2% uncertainties in load magnitude, Young's modulus, and mass density. Observe that in the bottom subplot, the uncertainties now do not increase over time, and the difference between IS and MC is much smaller than to top subplot. So it is indeed the increased number of interval variables that caused the increased uncertainty and the difference between IS and MC.

5. Conclusion

An interval finite element formulation is presented for the time-domain dynamic analysis of elastic structures with uncertain geometric and material properties. By using the Discrete Fourier Transform (DFT) and the Inverse Discrete Fourier Transform (IDFT), the given equivalent load and the final obtained structural responses are both given in the time domain, but the matrix inversion process is performed in the frequency domain. Ground motion and non-trivial initial conditions

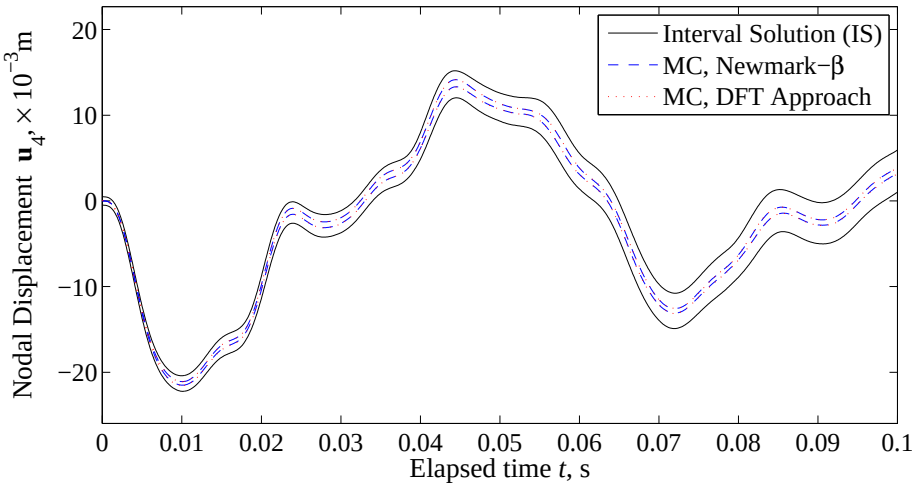

Figure 5. Lower and upper bounds of the nodal displacement $\mathbf{v}_5$ at joint 5 for the four-story frame of Figure 4 under external loads: IS (black solid lines) from the current method and MC predictions (blue dashed lines and red dotted lines) from an ensemble of 100,000 simulations. Parameter uncertainties are 1% for load magnitude, load history, Young's modulus, and mass density (see online version for colors).

are successfully handled via the introduction of the corresponding equivalent nodal forces. The resulting method is both efficient and widely applicable.

Uncertain parameters of the structure are modeled as intervals. The obtained interval enclosures guarantee to enclose the exact solution set with small overestimation, even for large uncertainty levels. Numerical examples show that the presented method gives guaranteed sharp bounds on the dynamic responses of the structure, even in cases when a large number of interval variables are present and other available methods give over-optimistic prediction on the lower and upper bounds.

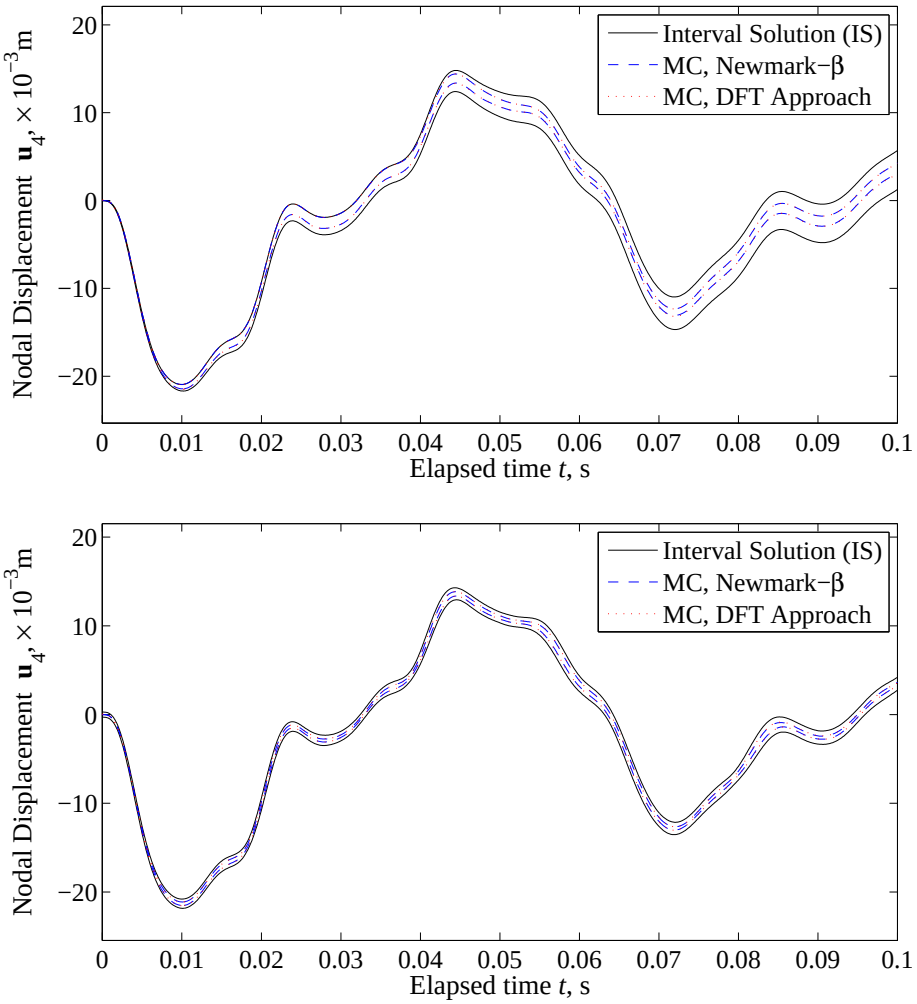

Figure 6. Lower and upper bounds of the nodal displacement $\mathbf{v}_5$ at joint 5 for the four-story frame of Figure 4 with: (top) 2% uncertainty only in load history; (bottom) 2% uncertainties in load magnitude, Young's modulus, and mass density. IS (black solid lines) from the current method and MC predictions (blue dashed lines and red dotted lines) from an ensemble of 100,000 simulations (see online version for colors).

References

Adhikari S. and H. H. Khodaparast. A spectral approach for fuzzy uncertainty propagation in finite element analysis. *Fuzzy Sets and Systems*, 243:1–24, 2014.

Alefeld, G. and J. Herzberger. *Introduction to Interval Computation*. Academic Press, 1984.

Bae, S. H., J. R. Cho, S. R. Bae and W. B. Jeong. A discrete convolutional Hilbert transform with the consistent imaginary initial conditions for the time-domain analysis of five-layered viscoelastic sandwich beam. *Computer Methods in Applied Mechanics and Engineering*, 268:245–263, 2014.

Bai, Y. C., C. Jiang, X. Han and D. A. Hu. Evidence-theory-based structural static and dynamic response analysis under epistemic uncertainties. *Finite Elements in Analysis and Design*, 68:52–62, 2013.

Corliss, G., C. Foley and R. B. Kearfott. Formulation for reliable analysis of structural frames. *Reliable Computing*, 13(2):125–147, 2007.

De Borst, R., M. A. Crisfield, J. J. C. Remmers and C. V. Verhoosel. *Nonlinear Finite Element Analysis of Solids and Structures*. John Wiley & Sons, 2012.

Dehghan, M., B. Hashemi and M. Ghatee. Computational methods for solving fully fuzzy linear systems. *Applied Mathematics and Computation*, 179(1):328–343, 2006.

Dempster, A. P. Upper and lower probabilities induced by a muilti-valued mapping. *The Annals of Mathematical Statistics*, 38:325–339, 1967.

Do, D. M., W. Gao, C. Song and S. Tangaramvong. Dynamic analysis and reliability assessment of structures with uncertain-but-bounded parameters under stochastic process excitations. *Reliability Engineering & System Safety*, 132:46–59, 2014.

Dokainish, M. A. and K. Subbaraj. A survey of direct time-integration methods in computational structural dynamics: I. Explicit methods. *Computers & Structures*, 32(6):1371–1386, 1989.

Erdogan, Y. S. and P. G. Bakir. Inverse propagation of uncertainties in finite element model updating through use of fuzzy arithmetic. *Engineering Applications of Artificial Intelligence*, 26(1):357–367, 2013.

Fernández-Martínez, J. L., Z. Fernández-Muñiz, J. L. G. Pallero, L. M. Pedruelo-González. From Bayes to Tarantola: new insights to understand uncertainty in inverse problems. *Journal of Applied Geophysics*, 98:62–72, 2013.

Hu, J. and Z. Qiu. Non-probabilistic convex models and interval analysis method for dynamic response of a beam with bounded uncertainty. *Applied Mathematical Modelling*, 34(3):725–734, 2010.

Igusa, T., S. G. Buonopane and B. R. Ellingwood. Bayesian analysis of uncertainty for structural engineering applications. *Structural Safety*, 24(2):165–186, 2002.

Impollonia, N. and G. Muscolino. Interval analysis of structures with uncertain-but-bounded axial stiffness. *Computer Methods in Applied Mechanics and Engineering*, 200(21):1945–1962, 2011.

Jiang, C., Z. Zhang, X. Han and J. Liu. A novel evidence-theory-based reliability analysis method for structures with epistemic uncertainty. *Computers & Structures*, 129:1–12, 2013.

Klir, G. J. and M. J. Wierman. *Uncertainty-Based Information - Elements of Generalized Information Theory*. Physica-Verlag, Heidelberg, 1999.

Kulisch, U. W. and W. L. Miranker. *Computer Arithmetic in Theory and Practice*. Academic Press, New York, 1981.

Lee, U., S. Kim and J. Cho. Dynamic analysis of the linear discrete dynamic systems subjected to the initial conditions by using an FFT-based spectral analysis method. *Journal of Sound and Vibration*, 288(1):293–306, 2005.

Liu, F., H. Li, W. Wang and B. Liang. Initial-condition consideration by transferring and loading reconstruction for the dynamic analysis of linear structures in the frequency domain. *Journal of Sound and Vibration*, 336:164–178, 2015.

Liu, G. and V. Kreinovich. Fast convolution and fast Fourier transform under interval and fuzzy uncertainty. *Journal of Computer and System Sciences*, 76(1):63–76, 2010.

Lutes, L. D. and S. Sarkani. *Random Vibrations: Analysis of Structural and Mechanical Systems*. Butterworth-Heinemann, 2004.

Mansur, W. J., J. A. M. Carrer, W. G. Ferreira, D. G. A. Claret and F. Venancio-Filho. Time-segmented frequency-domain analysis for non-linear multi-degree-of-freedom structural systems. *Journal of Sound and Vibration*, 237(3):457–475, 2000.

Moens, D. and M. Hanss. Non-probabilistic finite element analysis for parametric uncertainty treatment in applied mechanics: Recent advances. *Finite Elements in Analysis and Design*, 47(1):4–16, 2011.

Moore, R. E., R. B. Kearfott and M. J. Cloud. *Introduction to Interval Analysis*. Society for Industrial and Applied Mathematics, 2009.

Muhanna, R. L. and R. L. Mullen. Uncertainty in mechanics problems-interval-based approach. *Journal of Engineering Mechanics*, American Society of Civil Engineers, 127(6):557–566, 2001.

Muhanna, R. L., H. Zhang and R. L. Mullen. Combined axial and bending stiffness in interval finite-element methods. *Journal of Structural Engineering*, 133(12):1700–1709, 2007.

Paz, M. *Structural Dynamics: Theory and Computation*. Springer Science & Business Media, 1997.

Qiu, Z. and Z. Ni. An inequality model for solving interval dynamic response of structures with uncertain-but-bounded parameters. *Applied Mathematical Modelling*, 34(8):2166–2177, 2010.

Rump, S. M. *INTLAB - INTerval LABoratory*. Kluwer Academic Publishers, 77–104, 1999.

Santamarina, J. C. and D. Fratta. *Discrete Signals and Inverse Problems: an Introduction for Engineers and Scientists*. John Wiley & Sons, 2005.

Shafer, G. *A Mathematical Theory of Evidence*. Princeton University Press, Princeton, 1968.

Soize, C. Bayesian posteriors of uncertainty quantification in computational structural dynamics for low-and medium-frequency ranges. *Computers & Structures*, 126:41–55, 2013.

To, C. and W. Solomon. Response analysis of nonlinear multi-degree-of-freedom systems with uncertain properties to non-Gaussian random excitations. *Probabilistic Engineering*, 27(1):75–81, 2012.

Unger, J. F. and C. Könke. An inverse parameter identification procedure assessing the quality of the estimates using Bayesian neural networks. *Applied Soft Computing*, 11(4):3357–3367, 2011.

Veletsos, A. S. and A. Kumar. Steady-state and transient responses of linear structures. *Journal of Engineering Mechanics*, American Society of Civil Engineers, 109(5):1215–1230, 1983.

Veletsos, A. S. and C. E. Ventura. Dynamic analysis of structures by the DFT method. *Journal of Structural Engineering*, American Society of Civil Engineers, 111(12):2625–2642, 1985.

Xia, Y., Z. Qiu and M. I. Friswell. The time response of structures with bounded parameters and interval initial conditions. *Journal of Sound and Vibration*, 329(3):353–365, 2010.

Yang, Y., Z. Cai and Y. Liu. Interval analysis of dynamic response of structures using Laplace transform. *Probabilistic Engineering Mechanics*, 29:32–39, 2012.

Zhang, H. *Nondeterministic Linear Static Finite Element Analysis: an Interval Approach*. Georgia Institute of Technology, PhD Thesis, 2005.